



THE EFFECTS OF GEOMETRICAL CONFIGURATION ONTO MEASURING ENSEMBLE AVERAGED SURFACE NORMAL IMPEDANCE

Nazli bin Che Din^{1,2}, Toru Otsuru¹, and Reiji Tomiku¹

¹Department of Architecture and Mechatronics, Faculty of Engineering, Oita University, 700 Dannoharu, 870-1102 Oita, Japan

²Department of Architecture, Faculty of Built Environment, University of Malaya, Lembah Pantai, 50603 Kuala Lumpur, Malaysia
e-mail: nazli@cc.oita-u.ac.jp

Noriko Okamoto

Venture Business Laboratory, Oita University, Dannoharu, 870-1102 Oita, Japan

An *in situ* measurement technique of a material's surface impedance using ambient noise was proposed by some of the authors to offer the utilization in actual environment mainly in architectural acoustics. Furthermore, in the previous paper the theoretical development and concept of "Ensemble Averaged" surface normal impedance were summarized using the math-physical model based on the boundary element method (BEM) by the authors. This paper further elaborates on past discussions on the ensemble averaged surface normal impedance method of measuring surface impedance and the absorption coefficient of materials. In investigating the level of utility in various applications, the effects of source-receiver-sample geometrical configuration are presented both in simulation and measurement. Several measurements are conducted in two experimental rooms, *i.e.* reverberation room and anechoic room. The resulting absorption characteristics are examined to propose an appropriate measurement setting and demonstrate the accuracy and general utility of the method. Through the investigation, the applicability, reliability and robustness of the proposed method are revealed.

1. Introduction

Useful information on the performance of acoustics absorptive materials are frequently identified by their surface acoustical properties e.g. the impedance, the absorption and reflection coefficients, etc. It is important to note that for normal sound incidence, impedance tube method¹ have

been widely used in measuring the surface acoustical properties of materials. To address the disadvantages of the impedance tube method for oblique incidence measurement, the two- or multi-microphone free field measurement have been adopted. However, these methods did not correspond reasonably well with the products *in situ*.

The two-microphone technique and reflection method are the most common techniques for *in situ* measurement. Among reported in relevant studies, Garai² and Mommertz³ techniques are well documented in the literature⁴. Both techniques require the unwanted reflections from other surfaces need to be removed by time windowing. The separation of parasitic component can be extracted from the sufficient time windows. However, frequency resolutions in low frequencies are fraught difficulties if the time window is too short. Furthermore, considerable geometrical configuration e.g. sample-microphone-source, of the techniques is compromised by the edge reflections from the test surface. Large surfaces are needed; otherwise the diffraction of edges at low frequencies is significant to the measured values.

Nocke⁵ proposed an alternative: an area-averaged effective impedance to measure a material's absorption characteristics using a reflection method with a Maximum Length Sequential (MLS) signal. By using the spherical wave formulation, accurate results are archived down to 80 Hz, but this requires also a very large sample of 16 m² to prevent edge effects being significant.

In our previous paper⁶, the theoretical development and concept of ensemble averaged surface normal impedance at random incidences were given. As described in Ref. 6, several BEM simulations of glass wool both at normal and at random incidences showed that ensemble averaging decreases the interference effect caused mainly by the specimen's edges. Additionally, the ensemble averaged surface normal impedance at random incidence with anisotropic consideration^{7, 8} was shown to give an appropriate expected value of the surface normal impedance of the material.

However, applications in other situations i.e. *in situ* require careful consideration in some practical measurement details. Most of the *in situ* measurement techniques are still problematic for geometrical configuration such as practicality of the relative positioning of a sound source, microphone and sample, etc.

Aiming toward an efficient measurement technique, the authors use the combination of a microphone and a particle velocity sensor (pu-sensor⁹) to investigate different geometrical configurations in measuring the acoustics behaviours of absorptive material.

The following sections provide short descriptions of the ensemble averaged surface normal impedance and a basic technique to measure it using a pu-sensor. Then, the results of a series of simulations by using the BEM and corresponding measurements to archive the required considerable geometrical configuration of the technique are presented.

2. Short description of the method

2.1 Analysis model

In a previous paper⁶, the preliminary study using numerical simulation based on the BEM, both in normal incidence and random incidence has been presented. The results prove clearly that ensemble averaging decreases the interference effect caused mainly by the specimen's edge. Also, the BEM simulation with anisotropy consideration⁷ is compared with those by the measurement result and gives an appropriate expected values of the surface normal impedance of the glass wool.

An impedance $\langle Z_n \rangle$ is introduced comprising ensemble averaged impedance over such a sufficient number of incoherent sound sources P_S so as to expect random incidence as shown in Fig. 1(a). To derive the surface normal impedance of a material, the mirror image method¹⁰ is applied to analysis the model. Figure 1(a) shows Ω , (x, y, z) , and (r, θ, ϕ) respectively signify the upper half space, Cartesian, and polar coordinate of systems. The specimen with the area of $L_1 \times L_2$ surrounded by an infinite hard-plane are assumed to be as portrayed in the figure.

The following equations are expected to yield a statistically good approximation of the surface normal impedance and corresponding absorption coefficient of a specimen.

$$\langle Z_n \rangle = \frac{\langle p_{surf} \rangle}{\langle u_{n,surf} \rangle}, \quad (1)$$

$$\langle \alpha \rangle = 1 - \frac{|\langle Z_n \rangle - \rho c|}{|\langle Z_n \rangle + \rho c|}. \quad (2)$$

2.2 Numerical simulation outline

To clarify the effect from geometrical configuration of the method, we simulate the phenomena by which ensemble averaged impedance is to be measured using the procedure described in previous paper⁶. A series of sound pressure and particle velocity are calculated using commercial software of BEM (WAON ver. 3.1; Cybernet Inc.), then $\langle Z_n \rangle$ can be reduced using Eq. (1). Both pressures and particle velocities are calculated in the frequency domains of 100 Hz - 500 Hz at a 25 Hz interval and 500 Hz - 1000 Hz at 50 Hz interval. To realize the incidence based on plane-wave assumption in the estimation of surface impedance, simulations are performed with distance of sound source, r , located 500 m from center of specimen, unless stated otherwise.

2.3 Measurement outline

The measurements follow the basic procedure described in the previous paper¹¹ except that the sensor is not an array of microphones; instead, it is a pu-sensor (Fig.1 (b)). The measurements are conducted in reverberation room with non-parallel walls and with 168 m³ at the Oita University.

In the reverberation room, six loudspeakers (Fostex FE-103) mounted in small boxes to radiate incoherent pink noises. The pink noises are filtered to eliminate unnecessary frequency component and to focus on 100 Hz to 1000 Hz. A sub-woofer (JVC SX-DW77) is also added to increase the low frequency energy roughly below 200 Hz. Then, a pu-sensor is placed at the center of the specimen and the sensor's outputs are plugged into a 2ch Fast Fourier Transform instrument (FFT, SA-78; Rion Co. Ltd.). The FFT resolution is set to 1.25 Hz and a Hanning window is used. Measured data are averaged 150 times.

In the similar way of the previous paper¹¹ was set, pu-sensor is placed close to the specimen's surface at the default distance of $d = 10$ mm. Detailed discussion of the difference attributable to d is given the following sections. In a practical measurement, to achieve the enough averaging, we propose the following equation:

$$\langle Z_n \rangle = \frac{1}{N} \sum_N \frac{\langle \tilde{p} \rangle}{\langle \tilde{u}_n \rangle}. \quad (3)$$

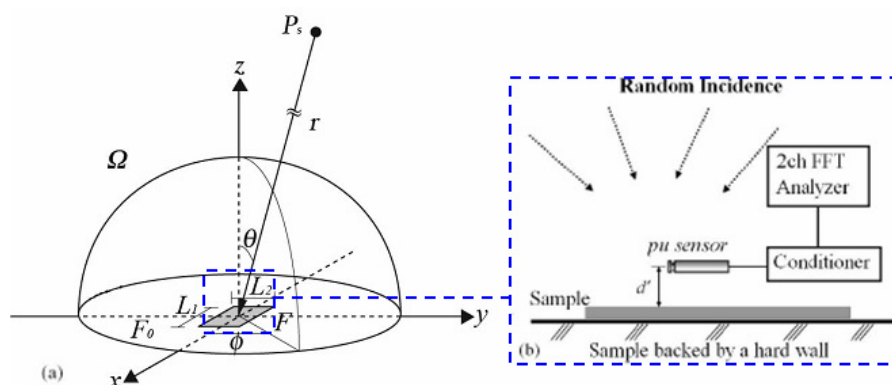


Figure 1. (a) System geometry and coordinates for a sound source P_s incident on a specimen F with the area of $L_1 \times L_2$ bounded by an infinitely flat hard plane F_0 ; (b) Block diagram of the measurement setup.

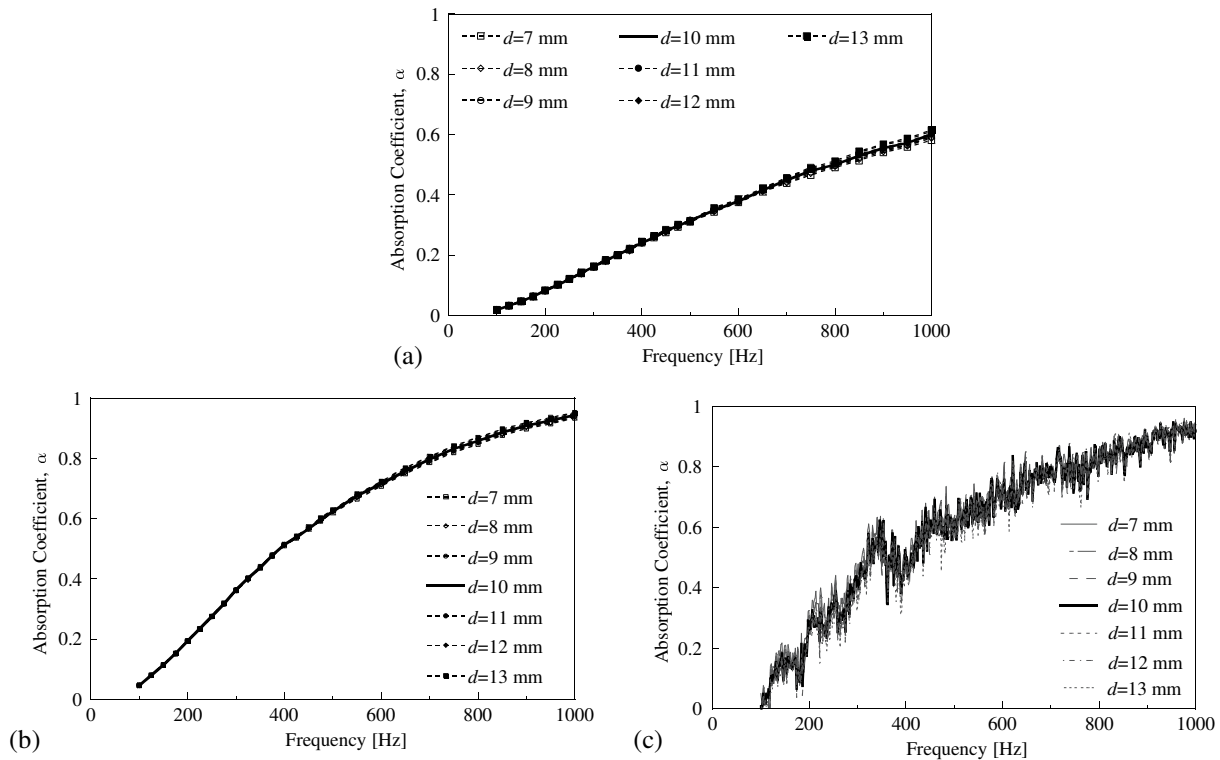


Figure 2. Comparisons of absorption coefficients of glass wool at random incidence with different sensor height: (a) simulated (GW25); (b) simulated (GW50); (c) measured (GW50).

3. Sensitivity test of geometrical configuration

So as to provide a condense presentation and ensure convenience for the reader, all the results are presented as absorption coefficients.

3.1 Influence of sensor distance

A series of BEM simulations is conducted to examine the effect of the sensor distance, d , onto the specimen's absorption characteristics. The sensor position is fixed at the center of specimen. Firstly, the setting of sensor height within ± 3 mm from the default setting, $d = 10$ mm, are simulated. Specimens to be analyzed are glass wool 25 mm thick (GW25) and glass wool 50 mm thick (GW50) with dimension L ($= L_1 = L_2$) = 1.0 m. Next, the effect of d when position heights are placed above from 10 mm with $d = 15, 20, 50, 100$ mm was also investigated. Specimens to be analyzed are GW50 with $L = 1.0$ and 2.0 m in sizes.

In the reverberation room, a series of measurement is conducted to obtain the sensor height effect onto absorption characteristics. The material of the specimen is the GW50 sized 1820 x 910 mm. The receiving point is fixed at the center of specimen with different setting of sensor height following BEM setting as mentioned above.

In Figs. 2(a) and 2(b), both simulation results showed no significant differences between the simulated absorption coefficients for different sensor heights. However, some discrepancies of absorption coefficient in frequency ranging from 800 Hz to 1000 Hz by about 0.02 can be observed in GW25. Moreover, the agreement between both the simulated and measured absorption coefficients of GW50 in Fig. 2(c) is sufficient to confirm that the differences of sensor height are negligible.

Next, the simulation results of corresponding absorption coefficients of each glass wool when $d = 10, 15, 20, 50$ and 100 mm are compared in Figs. 3(a) and 3(b). Despite the differences of specimen size, the corresponding absorption coefficients have the same tendency of differences when d become larger. The similar tendency outline of absorption coefficients of GW50 measurement results agree well with simulation results as shown in Fig. 3(c). In absorption coefficients results, the intensive fluctuations in the 800 Hz range and below are become highly evident when $d = 50$ mm

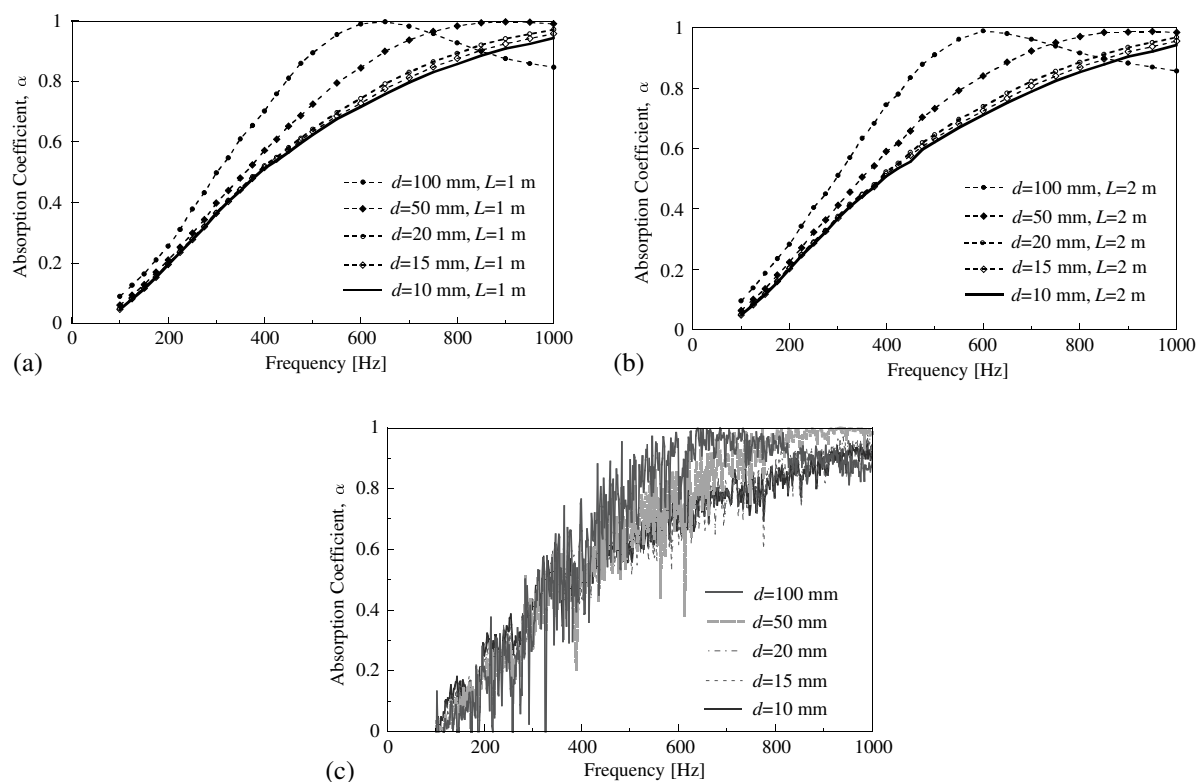


Figure 3. Comparisons of absorption coefficients of GW50 at random incidence with different sensor height: (a) simulated ($L = 1.0$ m); (b) simulated ($L = 2.0$ m); (c) measured.

and above which suggests the measurement might be not sufficiently effective for this range of sensor height.

3.2 Influence of sound source distance

In this section, we examine the effect of the sound source distance, r , for GW25, GW50 and additional of glass wool 100 mm thick (GW100) using the same BEM simulations settings. All specimens have similar size with $L = 1.0$ m. Again, using the procedure described above, we compare the simulated absorption coefficient of materials with $r = 500, 2.0, 1.0$ and 0.5 m. The sensor distance is fixed at the center of each specimen with $d = 10$ mm.

In Fig. 4(a), the effect is presented of the various distances between sound source and materials to the simulated absorption coefficients of the GW25, GW50 and GW100. All simulated absorption coefficients stay almost unchanged for each type of specimens except in simulated absorption coefficient of GW25 at 150 Hz and below, some discrepancies are apparent in the simulated result when $r = 0.5$ m. Following the solution of Nobile and Hayek¹² in calculating the surface impedance in normal incidence case, it may be safer to adopt $r = 1.0$ m and above. At this stage, we consider that the agreement is sufficient enough for the BEM simulation to investigate the phenomena.

3.3 Influence of incidence direction

Initially, point sources are located equally distributed 206 points on the sphere with $\phi = 0 - 360$ deg and resulting normalized impedances and absorption coefficients. In this investigation, the orientation of ϕ in BEM setting has been changed whilst maintaining the previous setting of the incidence angle ($\theta = 5 - 85$ deg at 10 deg interval) of the sound source. Four types of orientation direction ϕ s (0 deg, 0 - 45 deg, 0 - 90 deg, 0 - 180 deg) are examined with GW25, GW50 and GW100. All the specimens have the same square area with $L = 1.0$ m.

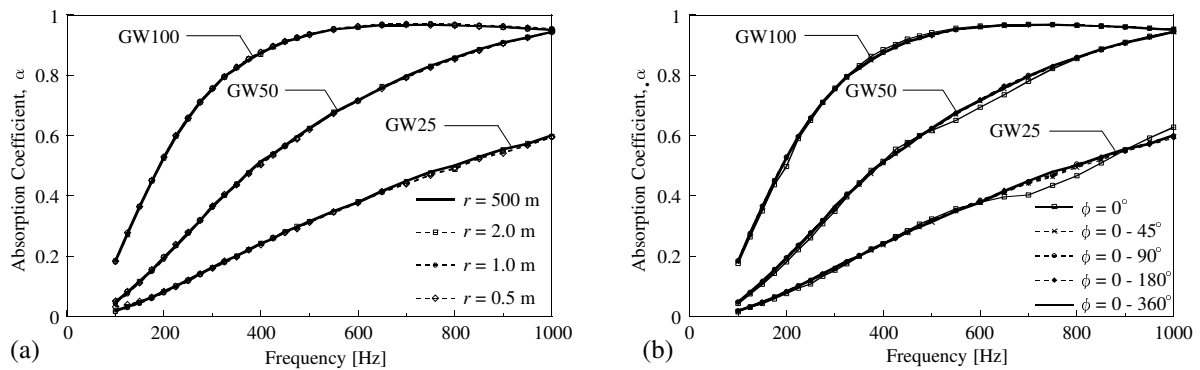


Figure 4. Comparisons of absorption coefficients of GW25, GW50 and GW100 at random incidence simulated by the BEM (a) Effects of source height; (b) Effect of the orientation of incident direction

As can be seen in Fig. 4(b), GW100 showed fair results in simulated absorption coefficient for each orientation of ϕ . Subsequently, similar tendency is obtained for both GW25 and GW50 except in the orientation of $\phi = 0$ deg, where some discrepancies are clearly apparent in corresponding absorption coefficients. It could be confirmed that the simulation with the rectangular or square shape of specimen requires incident direction, ϕ , of not less than 0 – 45 deg.

3.4 Influence of sample size

The investigation on finite sized surface will raise the issue of the measured area contributing to the total field. Garai² has suggested the easy way of reducing the minimum specimen size is to find a loudspeaker with very sharp impulse response but it not always economical. Also, the measurement becomes insufficient because too short time length of the window for the reflected pulse is needed which is about 0.01 s in radius 0.6 m of specimen.

To apply our method onto various practical measurements, the minimum measurable specimen's size must be clarified. A series of BEM simulations is conducted to examine the effect of the specimen size onto the specimen's absorption characteristics. Specimens to be analyzed are GW25, GW50 and GW100. All the specimens have the same square areas with $L = 1.0, 0.5, 0.3$ and 0.1 m where the receiving point is placed at the center of each specimen. A series of measurements is conducted to obtain absorption characteristics of specimens at random incidence condition. The material of the specimens is the GW50. Four sizes, $L = 0.9, 0.5, 0.3$ and 0.1 m, of specimens are measured and the receiving point $d = 10$ mm is fixed at the center of each specimens.

Comparisons of absorption coefficients obtained by the simulations for the specimens with the different sizes are given in Fig. 5(a). When simulated absorption coefficients of $L = 0.5, 0.3$ and 0.1 m are compared, the larger the L is, the higher the absorption coefficient becomes. There is no distinct difference between simulated absorption coefficients of $L = 0.5$ and 1.0 m. Moreover, excellent agreement of absorption coefficients for specimen above than $L = 1.0$ m are also confirmed.¹³

The results of the measurement are plotted in Fig. 5(b). The results of measured absorption coefficients show the tendency in the frequency range between 200 Hz and 800 Hz that the smaller the size is, the lower the absorption coefficient becomes, which corresponds with simulation findings. The agreement between the absorption coefficients of specimen with $L = 0.9$ m and 0.5 m is also confirmed as found in the simulation. The discrepancies in different specimen size can be regarded as mainly the result of reflections coming from around specimen.

4. Experimental confirmation

4.1 Measurement procedure

From the analysis of results described in the previous section, a series of measurements is conducted with 3 types of specimens in minimum measurable measurement setting condition. Glass

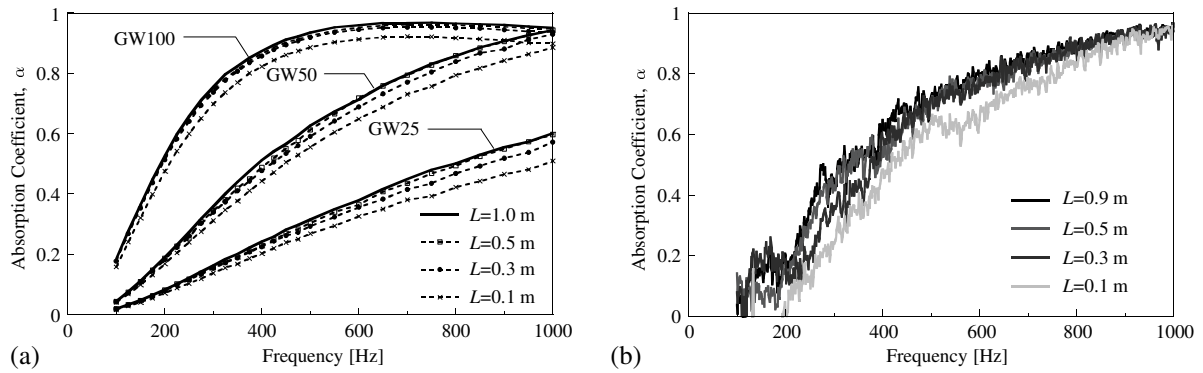


Figure 5. Comparisons of absorption coefficients of glass wool at random incident simulated by the BEM with respect to specimen's size: (a) simulated (GW25, GW50 and GW100); (b) measured (GW50)

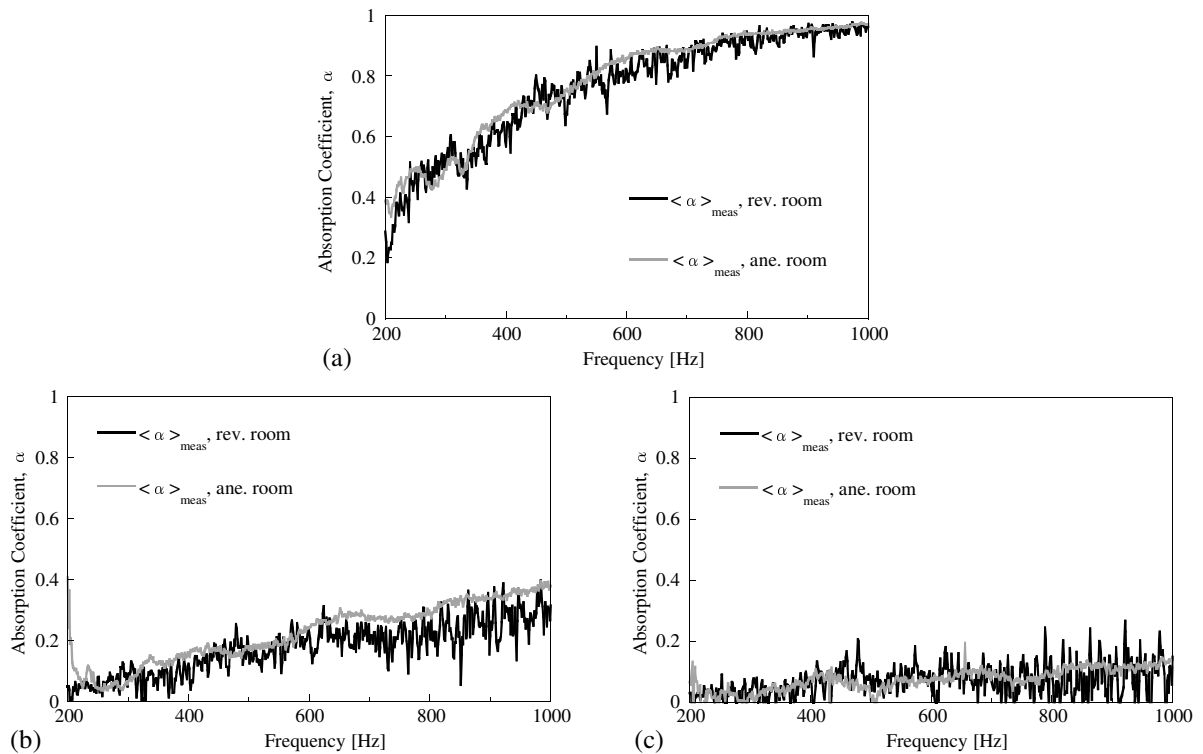


Figure 6. Comparisons of absorption coefficients of materials between by measured in a reverberation room and by measured in an anechoic room: (a) GW50; (b) NF; (c) TC.

wool (GW50), Needle Felt with 10 mm thick (NF10) and Tile Carpet (TC) are measured in anechoic room (58 m^3) at Oita University. All the specimens have the same square area with $L = 0.5 \text{ m}$. Receiving point is fixed at the center with $d = 10 \text{ mm}$ and sound source distance r is placed approximately 1.0 m from the center of specimens. The 10 cm single-cone speaker in a box was used and manually moved within range of the orientation almost in direction of $\phi = 0 - 45 \text{ deg}$. Next, the same materials are measured in the reverberation room with the same geometrical configuration as is described above except for the sound sources as are described in Sec. 2.3.

4.2 Measurement results

In Fig. 6, the corresponding absorption coefficients of each specimen measured in anechoic room are compared to those measured in the reverberation room. The absence of the woofer in both measurements shifts the focus of the frequency range from $100 \text{ Hz} - 1000 \text{ Hz}$ to $200 \text{ Hz} - 1000 \text{ Hz}$. Although, some discrepancy can be found in all specimens, the agreement of absorption coefficients gives plausible tendency at this stage of our study.

5. Conclusions

In this study, the geometrical configurations of ensemble averaged of normal surface impedance method have been presented by BEM and corresponding measurement. Although the minimal measurable setting is used, the presented results lead to the conclusion that reasonably accurate and effective measurements can be performed with this method. Further numerical and experimental investigations are now being pursued intensively, inter alia, on how to realize the randomness in practical measurements, on applications in various environments or on the applications onto computational simulations and on the reproducibility of the measured data.

6. Acknowledgements

This research is partially supported by a Japan Society for the Promotion of Science (JSPS), Grant-in-Aid for Exploratory Research, 19656143, 2007–9, and was conducted as one Research Project (A) of the Venture Business Laboratory in Oita University.

REFERENCES

- [1] ISO 10534, “Acoustics – Determination of sound absorption coefficient and impedance in impedance tubes -, Part 1 and 2,” (198).
- [2] M. Garai, “Measurement of the sound-absorption coefficient *in situ*: The reflection method using periodic pseudo-random sequences of maximum length,” *Applied Acoustics* **39**, 119-139 (1993).
- [3] E. Mommertz, “Angle-dependent in-situ measurements of reflection coefficients using a subtraction technique,” *Applied Acoustics* **46**, 251-263 (1995).
- [4] ISO 13472 Acoustics – Measurement of sound absorption properties of road surfaces *in situ* -, Part 1: Extended surface method,” (2002).
- [5] C. Nocke, “In-situ acoustic impedance measurement using a free-field transfer function method,” *Applied Acoustics* **59**, 253-264 (2000).
- [6] T. Otsuru, R. Tomiku, NBC Din, N. Okamoto and M. Murakami, “Ensemble averaged surface normal impedance of material using *in situ* technique: Preliminary study using boundary element method,” *Journal of Acoustical Society of America* **6**, 3784-3791 (2009).
- [7] J.F. Allard, R. Bourdier and A. L'Esperance, “Anisotropy effect in glass wool on normal impedance in oblique incidence,” *Journal of Sound and Vibration* **114**, 233-238 (1987).
- [8] J.S.Pyett, “The acoustic impedance of a porous layer at oblique incidence,” *Acustica* **3**, 375-382 (1953).
- [9] H.-E. de Bree, P. Leussink, T. Korthorst, H. Jansen, T. Lammerink and M. Elwenspoek, “The Microflow: A novel device measuring acoustical flows,” *Sensors and Actuators A SNA054/1-3*, 552-557 (1996).
- [10] Y. Kawai and H. Meotoiwa, “Estimation of area effect of sound absorbent surfaces by using a boundary integral equation,” *Acoustical Science and Technology* **26**, 123-127 (2005).
- [11] Y. Takahashi, T. Otsuru and R. Tomiku, “*In situ* measurements of surface impedance and absorption coefficients of porous materials using two microphones and ambient noise,” *Applied Acoustics* **66**, 845-865 (2005).
- [12] M. A. Nobile and S. I. Hayek, “Acoustic propagation over an impedance plane,” *Journal of Acoustical Society of America* **78**, 1325-1336 (1985).
- [13] T. Otsuru, Nazli bin Che Din, R. Tomiku, N. Okamoto, A. Kusno, “Setting for measuring ensemble averaged surface normal impedance,” *Proceeding of INTER-NOISE 2009*, (Ottawa, Canada), on CD-ROM.